

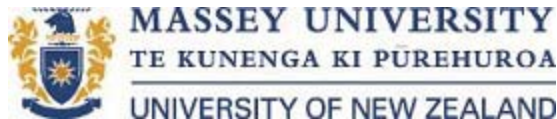
Copyright is owned by the Author of the thesis. Permission is given for a copy to be downloaded by an individual for the purpose of research and private study only. The thesis may not be reproduced elsewhere without the permission of the Author.

**High-precision tephrostratigraphy:  
Tracking the time-varying eruption pulse  
of Mt. Taranaki, North Island,  
New Zealand**

**A thesis presented in partial fulfilment of the  
requirements for the degree of**

**Doctor of Philosophy  
in  
Earth Science**

**at Massey University, Palmerston North, New Zealand.**



**Magret Damaschke**

**2017**



*Mt. Taranaki and the Ahukawakawa Swamp viewed from the Pouakai Tarns,  
North Island, New Zealand. (December 2014)*

---

## Abstract

In this research it was proposed that a more robust record of volcanic activity for Mt. Taranaki (New Zealand) could be derived from tephra (pyroclastic fall deposits) within cores from several lakes and peatlands across a 120° arc, NE-SE of the volcano, covering a range of prevailing down-wind directions. These data were integrated with previous tephrochronology studies to construct one of the longest and most complete volcanic eruption history records ever developed for an andesitic stratovolcano. Using 44 new radiocarbon dates, electron microprobe analysis of glass shard and titanomagnetite chemical composition, along with whole-rock chemistry, a chrono- and chemostratigraphy was established. The new record identifies at least 272 tephra-producing eruptions over the last 30 cal ka BP. Six chemo-stratigraphic groups were identified: A (0.5 – 3 cal ka BP), B (3 – 4 cal ka BP), C (4 – 9.5 cal ka BP), D (9.5 – 14 cal ka BP), E (14 – 17.5 cal ka BP), and F (23.5 – 30 cal ka BP). These were used to resolve previous stratigraphic uncertainties at upper-flank (proximal) and ring-plain (medial) sites. Several well-known “marker tephra” are now recognized as being ~2000 years older than previously determined (e.g., Waipuku, Tariki, and Mangatoki Tephra units) with the prominent Korito Tephra stratigraphically positioned above the Taupo-derived Stent Tephra. Further, new markers were identified, including the Kokowai Tephra unit (~4.7 cal ka BP), at a beach-cliff exposure, 40-km north-east of the volcano. Once age-models were established for each tephra, units were matched between sites using statistical methods. Initial statistical integration showed that the immediate past high-resolution tephrochronological record suffered from a distinctive “old-carbon” effect on its ages (Lake Rotokare). This had biased the most recent probabilistic forecasting and generated artificially high probability estimates (52-59% eruption chance over the next 50 years). Once the Rotokare record was excluded and chemostratigraphy constraints were applied, a reliable multi-site tephra record could be built only for the last ~14 ka BP. The new data confirms a highly skewed distribution of mainly (98% of cases) short intervals between eruptions (mode of ~9 years and average interval ~65 years). Long intervals (up to 580 years) as seen in earlier records were reduced to 2% of the record, but can now be considered real, rather than missing data.

The new data confirm a cyclic pattern of varying eruption frequency (with a five-fold range in annual frequency) on a period of ~1000-1500 years. The new time-varying frequency estimates suggest a lower probability for a new eruption at Mt. Taranaki over the next 50 years of 33-42%. The newly established chemostratigraphy was further used to investigate time-related compositional changes. Whole-lapilli analyses highlighted that a specific very evolved Ca-rich and Fe-poor composition was only found within the easterly and south-easterly depositional sites. This was explained by eruption of a stratified magma reservoir, which holds greater modal proportions of plagioclase and lower proportions of pyroxene within low-density, gas-rich upper conduit regions. During the most explosive phases of eruptions, when plumes reach the stratospheric jet-stream, the lowest-density pumice is thus dispersed by high-level stable westerly winds. Further, two distinct evolutionary trends were seen in the long and new tephrochronological record; from 17.5 to 3 cal ka BP and <3 cal ka BP; with whole-lapilli, glass, and titanomagnetite compositions overall evolving over time. The former compositional trend indicates a crystallising and cooling magma source in the deep crust, with multiple, spatially separated magma source regions forming, each generating magmas (i.e., magma batches) with unique titanomagnetite compositions. This trend is interrupted by a distinct shift towards less-evolved compositions and the initiation of a second parasitic vent (Fanthams Peak at the southern flank of Mt. Taranaki).

## Acknowledgements

Firstly, I would like to thank my chief supervisor, Prof. Shane J. Cronin (Auckland University) for giving me the opportunity of this PhD and for believing in me in the first place. He guided me throughout this thesis with constructive discussions and feedbacks as well as helping me receive a Massey Doctoral scholarship and the George Mason Charitable Trust scholarship. I also benefited greatly from his extraordinary skills in writing and presenting research papers.

I also wish to thank my co-supervisors Dr. Katherine A. Holt (Massey University), Assoc. Prof. Georg F. Zellmer (Massey University), and Prof. Mark S. Bebbington (Massey University) for the time, support and sheer enthusiasm that you have provided for this project and me. In particular, Dr. Holt is sincerely thanked for her assistance in the field and helpful introduction to various sediment coring procedures. I particularly thank Prof. Bebbington for his expertise and knowledge in the (to me unknown) field of statistics and Assoc. Prof. Zellmer for his guidance regarding my understanding of geochemical processes.

This thesis would not have been possible without the great support and encouragement of two very important people, who have become dearest friends over the past years:

Dr. Clel Wallace (Massey University) – I find it extremely difficult to express my gratitude and appreciation for all that you have done for me during my PhD years. You have not just provided me with knowledge, fruitful discussions, constructive criticism, spelling and grammar checks, excellent reviews, and lots of motivation related to my research, but also welcomed me into your lovely family. I will always cherish the evenings full of good food, plenty of wine and wonderful companions. Please deliver a special thanks to Nicky, and give Topsy & Misty a big hug.

AND

Rafael Torres-Orozco (Massey University) – I would like to thank you for being my best colleague and incognito-supervisor over the course of my PhD. You taught me a lot, professionally and personally, inspired me with new ideas, provided me with a good

deal of patience and time, and always believed in me. Your enthusiasm for volcanology and Mt. Taranaki has had me enthralled. I thank you so much for the numerous times we tried to unravel this monstrosity of a volcano together, climbed his steep flanks not just for work, and occupied long overtime hours accompanied with productive discussions and a high-level coffee consumption.

Special thanks also goes to Mr. David Feek (Massey University), who contributed greatly to many successful coring campaigns by providing his technical skills and excellent sense of humour; and to Dr. Anja Moebis (Massey University) and Mr. Peter Lewis (Massey University) for their helpful instructions and support during laboratory and analytical works. I would also like to thank Dr. Alan Palmer (Massey University) for his field assistance, and Assoc. Prof. Robert B. Stewart (Massey University) for his fruitful discussions regarding the petrology and geochemistry of Mt. Taranaki eruptives as well as helpful introduction and assistance in X-ray powder diffraction (XRD) analysis. I am also very grateful to Prof. Vince E. Neall (Massey University), who's unlimited enthusiasm for, and knowledge about, Mt. Taranaki over so many years inspired and encouraged me throughout my own PhD years. He is also thanked for providing me with previous field samples, notes and ideas, which contributed greatly to my research. I also wish to thank Assoc. Prof. Alan Hogg and Dr. Fiona Petchey (Waikato University) for radiocarbon dating multiple sediment samples during my research, and for your fast response and accuracy.

I want to acknowledge all of those who have assisted me during my research: Thank you Dr. Kate Arentsen (Massey University) for organising hotel and car bookings during my field trips and being able to help me with any administrative concerns. I also would like to thank Assoc. Prof. Ian Smith (Auckland University) for his help and time during the evaluation and interpretation of the geochemical analyses; in particular of the laser ablation–inductively coupled plasma–mass spectrometry (LA-ICP-MS) titanomagnetite data. Mr. Ian Furkert and Mr. Bob Toes (Massey University) are thanked for their assistance within the laboratories, and their reassuring kindness although I almost set the lab on fire once. I am also very grateful to Ms. Julie Palmer (Massey University) and her family, who gave me great support and the opportunity to follow my passion for horse riding. I am grateful to the whole Volcanic Risk Solution

department (Massey University), including Assoc. Prof. Jonathan Procter, Assoc. Prof. Karoly Nemeth, Dr. Gert Lube and colleagues/friends Ermanno Brosch, Marija Voloschina, Kevin Kreutz, Gaby Gomez, Gabor Kereszturi, Szabolcs Kosik for their support and encouragement. I also wish to thank Prof. David J. Lowe (Waikato University), Dr. Alastair Clement (Massey University), and Dr. Victoria C. Smith (Oxford University) for examining my thesis and their helpful comments and feedback.

Many thanks also go to Taranaki landowners Steve Styger, Gary Comarer, Trevor Jane, John & Jack Newsome, Raymond Foster, Brian Rowlands, Alison Rumball, and the Tamblin family for allowing access to their properties for sampling and their unreserved trust in this project.

And lastly, but most importantly, I owe everything to my friends and family back in Germany. My sincere thanks go to my parents, grandparents and my brother, who always supported me in everything I pursued. Your love, care, and understanding is priceless. I could not have done this without you. To my dearest friends, Yvonne Baumann and Julia Pauli, thank you so much for your moral support and unconditional friendship.

This thesis is dedicated to my grandpa, who unexpectedly past away during my stay here in New Zealand. I love you Opi.



# Table of contents

Abstract.....	i
Acknowledgements.....	iii
Table of contents.....	vi
List of tables.....	xi
List of figures.....	xiii

## **Chapter 1 ..... 1**

Introduction.....	1
1.1 Introduction .....	1
1.2 Objectives .....	3
1.3 Background geology.....	5
1.3.1 Regional setting .....	5
1.3.2 Taranaki setting.....	7
1.3.3 The volcanic eruption history of Mt. Taranaki .....	10
1.3.4 Petrology and geochemistry of Mt. Taranaki .....	11
1.3.5 Previous tephrostratigraphy at Mt. Taranaki .....	12
1.3.6 Volcanic hazard at Mt. Taranaki.....	18
1.4 Background geography.....	21
1.4.1 Physiography.....	21
1.4.2 Climate.....	21
1.4.3 Vegetation and soils.....	22
1.4.4 Palaeoclimate .....	24
1.5 Study sites.....	29
1.6 Thesis outline.....	32
1.7 References .....	33

## **Chapter 2 ..... 49**

Methodology .....	49
2.1 Field study .....	49

2.1.1	Field sampling and core processing .....	49
2.1.2	Core shortening .....	52
2.2	Laboratory procedures .....	55
2.2.1	Sample preparation .....	56
2.2.2	Composite cores .....	56
2.2.3	Radiocarbon dating .....	57
2.2.4	Grain-size .....	59
2.2.5	X-ray diffraction (XRD) .....	59
2.2.6	Electron probe micro-analyzer (EPMA) .....	60
2.2.6.1	Limitations .....	61
2.2.6.2	Geochemical outliers .....	62
2.2.7	X-ray fluorescence (XRF) spectrometry and laser ablation–inductively coupled plasma–mass spectrometry (LA-ICP-MS) .....	64
2.3	References .....	65

## **Chapter 3 ..... 69**

Tephrostratigraphy of lake and peat sediment records from Mt. Taranaki, New Zealand .....		69
3.1	Introduction .....	70
3.2	A 30,000-year high-precision eruption history for the andesitic Mt. Taranaki, North Island, New Zealand .....	71
3.2.1	Abstract .....	71
3.2.2	Introduction .....	72
3.2.3	Study sites .....	74
3.2.4	Methods .....	76
3.2.4.1	Field sampling and core processing .....	76
3.2.4.2	Radiocarbon dating .....	77
3.2.4.3	Grain-size and geochemistry .....	79
3.2.4.4	Depth information .....	80
3.2.5	Results .....	81
3.2.5.1	Age-depth models .....	81
3.2.5.2	Core descriptions .....	83

3.2.5.3	Titanomagnetite groups.....	91
3.2.5.4	Glass chemistry .....	94
3.2.5.5	Discrimination of tephra sequences .....	97
3.2.6	Discussion.....	108
3.2.6.1	Correlation using defined tephra sequences.....	108
3.2.6.2	Tephra deposition/preservation.....	110
3.2.6.3	Preliminary implications for Mt. Taranaki's magmatic system.....	112
3.2.7	Conclusions.....	114
3.2.8	Acknowledgements.....	115
3.2.9	References.....	116

## **Chapter 4 ..... 124**

A proximal-distal tephra correlation of andesitic tephra deposits from Mt. Taranaki, New Zealand..... 124

4.1 Chapter synopsis..... 124

4.2 Unifying tephrostratigraphic approaches to redefine major Holocene marker tephra, Mt. Taranaki, New Zealand ..... 126

4.2.1 Abstract..... 126

4.2.2 Introduction..... 127

4.2.3 Previous tephrostratigraphy ..... 130

4.2.4 Sites and samples ..... 136

4.2.4.1 Flank localities (proximal) ..... 136

4.2.4.2 Ring-plain localities (medial)..... 136

4.2.5 Methods..... 137

4.2.6 Results..... 139

4.2.6.1 Titanomagnetite and glass chemistry of proximal deposits on the flanks..... 139

4.2.6.2 Onaero Beach section..... 144

4.2.6.3 Mangatoki Stream section..... 145

4.2.7 Discussion..... 147

4.2.7.1 Correlating proximal and medial deposits with dated tephra sequences from lake and peat records ..... 147

4.2.7.2	Implications for andesitic tephra correlation.....	159
4.2.8	Conclusions.....	161
4.2.9	Acknowledgements.....	162
4.2.10	References.....	163

## **Chapter 5 .....172**

Probabilistic eruption forecasting using a multi-site high-resolution tephra record from Mt. Taranaki, New Zealand .....		172
5.1	Chapter synopsis.....	172
5.2	Using multi-site tephra records to develop volcanic eruption frequency models and hazard estimates, Mt. Taranaki, New Zealand .....	174
5.2.1	Abstract.....	174
5.2.2	Introduction.....	175
5.2.3	Eruption frequency.....	178
5.2.3.1	Single records.....	178
5.2.3.2	Merged records.....	182
5.2.4	Hazard modelling.....	188
5.2.4.1	Temporal models.....	188
5.2.4.2	Probabilistic eruption forecasting.....	190
5.2.5	Discussion and conclusions .....	195
5.2.6	Acknowledgements.....	198
5.2.7	References.....	198

## **Chapter 6 .....205**

Geochemical variation of tephras from Mt. Taranaki, New Zealand: Implications for magma evolution.....		205
6.1	Chapter synopsis.....	205
6.2	Introduction .....	206
6.2.1	Andesitic volcanism.....	208
6.2.2	Previous petrographic and geochemical work at Mt. Taranaki .....	209
6.2.3	Basement geology and xenoliths .....	210
6.3	Methods .....	211

6.4	Results .....	213
6.4.1	Whole-lapilli compositions.....	213
6.4.2	Glass shard compositions.....	221
6.4.3	Titanomagnetite compositions.....	221
6.4.4	Temporal variation of whole-lapilli, glass shard, and titanomagnetite compositions .....	226
6.4.4.1	Whole-lapilli and glass shard compositional variations.....	226
6.4.4.2	Titanomagnetite compositional variations .....	227
6.5	Discussion.....	231
6.5.1	Contrasting whole-lapilli compositions .....	231
6.5.2	Fractionation trends .....	233
6.5.3	Compositional variations: Implication for Mt. Taranaki's magmatic system .....	238
6.5.3.1	Whole-lapilli and glass trends .....	238
6.5.3.2	Titanomagnetite trends.....	239
6.5.3.3	An exploratory study of the use of LA-ICP-MS techniques to fingerprint titanomagnetites .....	242
6.6	Conclusions .....	243
6.7	References .....	244

## **Chapter 7 .....257**

Conclusions and future work .....	257
7.1 Conclusions .....	257
7.2 Future work.....	260
7.3 References .....	262

## **List of appendices.....265**

## List of tables

<b>Table 2. 1</b> <i>Field expeditions and recovered sediment cores during this study. ....</i>	51
<b>Table 2. 2</b> <i>Detection limits of element oxides measured at the electron microprobe (University of Auckland) including the deviation from a reference glass composition..</i>	61
<b>Table 3. 1</b> <i>Radiocarbon ages acquired from lake and peat sediment cores recovered during this study.....</i>	78
<b>Table 3. 2</b> <i>Compositions of 12 individual titanomagnetite (tm) groups recognised in tephra layers from lake and peat sediment records at Mt Taranaki. Refer also to Figure 3.7. *Additional analyses of grey lapilli tephra layer within the Eltham Swamp core recovered by McGlone and Neall (1994).....</i>	93
<b>Table 4. 1</b> <i>Current proximal tephrostratigraphy and relevant radiocarbon dates at Mt Taranaki.....</i>	134
<b>Table 4. 2</b> <i>The marker tephra units from Mt. Taranaki analysed in the current study.</i>	137
<b>Table 4. 3</b> <i>Summary of the titanomagnetite groups defined by Damaschke et al. (2017) and associated proximal and medial deposits analysed in the current study.....</i>	141
<b>Table 5. 1</b> <i>Correlations used in the merging algorithm (c.f., Green et al. 2014). They are based on the physical and geochemical characteristics of the tephra, as well as, on their stratigraphic position and age constraints (implemented by Damaschke et al. 2017a). ....</i>	187
<b>Table 5. 2</b> <i>Fitted parameters and average log-likelihoods for the models tested for both of the last explosive eruptions of Mt. Taranaki at AD1785 and AD1820.....</i>	191
<b>Table 6. 1</b> <i>Whole-lapilli composition for Upper Inglewood distal and proximal tephra. ....</i>	233

**Table 6. 2** *Fractional crystallisation modelling of tephra chemistry at Mt. Taranaki.* 235

## List of figures

- Figure 1. 1** *Plate tectonic setting of New Zealand (modified after Chanier et al., 1999). Arrows indicate plate motion of the Pacific Plate relative to the Indo-Australian Plate with rates adopted from DeMets et al. (1994) and Beavan et al. (2002). The Taupo Volcanic Zone (TVZ) and Mt. Taranaki are also shown. .... 6*
- Figure 1. 2** *Tectonic and volcanological setting of the North Island of New Zealand (modified after Price et al., 1999). The Taranaki Volcanic Lineament encompassing Mt. Taranaki (T), Pouakai Volcano (P), Kaitake Volcano (K), and the Sugar Loaf Islands and Paritutu (S). The Taupo Volcanic Zone (TVZ) encompassing Ruapehu Volcano (R), Mt. Ngauruhoe (N), Mt. Tongariro (To), Lake Taupo (Tau), Maroa Volcano (Ma), Mt. Tarawera (Ta), Mt. Edgecumbe (E), and White Island (W). The Alexandra Volcanic Lineament (Briggs et al., 1989) is also shown. Contours show depth to the Wadati–Benioff Zone (Boddington et al., 2004; Reyners et al., 2006, 2011). .... 8*
- Figure 1. 3** *Volcanic, volcanoclastic and sedimentary deposits shown in the quaternary geological map of Mt. Taranaki (modified after Neall and Alloway, 2004). Sediment coring locations of previous studies (Lees and Neall, 1993; McGlone and Neall, 1994; Turner et al., 2008a, 2009) including the Eltham Swamp (ES), Ngaere Swamp (NS), Midhirst Swamp (MS), Lake Umutekai (LU) and Lake Rotokare (LRk) are also shown. .... 10*
- Figure 1. 4** *(1) Volcanic hazard zones for on-ground-type events for the Taranaki region (from Neall and Alloway, 1995). (2) Tephra fall hazard zones (A-D) from future eruptions of Mt. Taranaki (from Neall and Alloway, 1993). Expected thickness for tephra in zone A greater than 25 cm, in zone B between 25-10 cm, in zone C between 10-1 cm, and in zone D between 1-0.1 cm. .... 20*
- Figure 1. 5** *(A) landforms of the Taranaki region (Taranaki Regional Council, 2014), (B) Taranaki median annual average temperature (NIWA, 2014), (C) Taranaki median annual total rainfall (NIWA, 2014). .... 22*



**Figure 1. 6** *Vegetation-profile of the Taranaki region (after Newnham and Alloway, 2004).* ..... 23

**Figure 1. 7** *The NZ-INTIMATE climate event stratigraphy (after Barrell et al., 2013 and Alloway et al., 2007).* ..... 27

**Figure 1. 8** *Location map of the study sites. Peatlands are highlighted by the orange fields; whereas stars represent specific coring location. Lakes are also indicated by stars, whereas green stars indicate previous (pv) coring sites of Turner et al. (2008a, 2009). Note the change in physiographic textures, which is the contrast between the smooth volcanic ring-plain to the west and the dissected mudstone hill country to the east.* ..... 31

**Figure 2. 1** (A) *Illustration of the coring procedure at peat sites, using a percussion coring system. Note (1) that the first core extracted has a total length of 1.06 m, (2) while following cores are of 1-metre lengths with 0.94 m of sediment within the PVC-liner and 6 cm within the core-cutter. (B) Shows the hydraulic percussion coring system used in the field (identified by the Roman numerals in white I, II & III): (I) petrol-driven percussion hammer, (II) steel core-barrel with inserted 1 m-long PVC-liner, and (III) hydraulic jack.*..... 50

**Figure 2. 2** (A) *Shows the raft and the equipment used for coring the lake sediments. (B) Illustrates the jack, which was required to lift Livingston piston-corer from the lake bottom with technician David Feek. The lake shown in both images is Lake Richmond, which was first cored during this study. (C) Diagram from Woodward and Sloss (2013) showing the piston corer components similar to that used during this study, and its coring operation with (1) the corer positioned above the sediment surface and (2-3) subsequently pushed into the soft sediments, while simultaneously keeping the core-cable tight so as to create suction until the desired depth has been penetrated, (4) the corer extracted with the sediments.* ..... 51

**Figure 2. 3** *Diagram from Morton and White (1997) showing core shortening patterns in unconsolidated sediments: (a) no shortening (very rare), (b) uniform shortening*

(rare), (c) systematic increased shortening (common), (d+e) mixed pattern shortening (very common). .....	53
---	----

<b>Figure 2. 4</b> Interval (%) and cumulative (cm) shortening of individual sediment cores taken during this study. ....	54
---	----

<b>Figure 2. 5</b> Flowchart illustrating the methodology that was implemented in this study. Abbreviations for analytical methods as follows: AMS = Accelerator Mass Spectrometry, X-ray = X-radiography, XRD = X-ray diffraction, LPA = Laser Particle Analyser, EPMA = Electron Probe Micro-Analyser, XRF = X-ray fluorescence spectrometry, LA-ICP-MS = laser ablation-inductively coupled plasma-mass spectrometry.....	55
--	----

<b>Figure 3. 1</b> Age-depth models for lake and peat sediment cores, produced using a piecewise cubic Hermite interpolating polynomial fit (Fritsch and Carlson, 1980). Individual <sup>14</sup> C ages are shown as calibrated median probability ages with 1σ errors output by OxCal Version 4.2 (Bronk Ramsey, 2013) (Table 3.1). The s.depths are shown as "event-free" depths. Sediment accumulation rates are given as mm/yr. Brief lithologies are also shown. The red star indicates an accumulation increase around 5-5.5 cal ka BP within Lake Richmond and Lake Umutekai. Three Taupo volcano tephra layers are recognised and dated: (1) Stent Tephra (mean age from Lake Richmond: 4279±47 cal yr BP, age from Lake Umutekai: 4296±92 cal yr BP; age from Lake Rotokare: abnormal), (2) Kawakawa Tephra (age from Eltham Swamp: 25,447±125 cal yr BP) and (3) Okaia Tephra (age from Eltham Swamp: 28,735±143 cal yr BP). .....	82
---	----

<b>Figure 3. 2</b> Lake Richmond sediment cores recovered during this study (R1-R3) and the composite record. Images show prominent tephra layers and their juvenile clast assemblages. Key correlations are marked with dotted red lines and are based on physical characteristics and age. Reworked tephras are abbreviated as 'rew.'. Ages are shown as calibrated ages with 1σ errors (Table 3.1). ....	84
---	----

<b>Figure 3. 3</b> Tariki Swamp sediment cores recovered during this study (T1-T2) and the composite record. Images show prominent tephra layers and their juvenile clast	
---	--

*assemblages. Key correlations are marked with dotted red lines and are based on physical characteristics and age, while dotted purple correlation-lines are additionally based on geochemical characteristics. Reworked tephras are abbreviated as 'rew.'. Ages are shown as calibrated ages with  $1\sigma$  errors (Table 3.1). ..... 86*

**Figure 3. 4** *Ngaere Swamp sediment cores recovered during this study (N1-N2) and the composite record. Images show prominent tephra layers and their juvenile clast assemblages. Key correlations are marked with dotted red lines and are based on physical characteristics and age, while dotted purple correlation-lines are additionally based on geochemical characteristics. Reworked tephras are abbreviated as 'rew.'. Ages are shown as calibrated ages with  $1\sigma$  errors (Table 3.1). ..... 88*

**Figure 3. 5** *Eltham Swamp sediment cores recovered during this study (E1-E2) and the composite record. Images show prominent tephra layers and their juvenile clast assemblages. Key correlations are marked with dotted red lines and are based on physical characteristics and age, while dotted purple correlation-lines are additionally based on geochemical characteristics. Reworked tephras are abbreviated as 'rew.'. Ages are shown as calibrated ages with  $1\sigma$  errors (Table 3.1). ..... 90*

**Figure 3. 6** *Compositions of titanomagnetite phenocrysts recognised in lake and peat deposits of Mt. Taranaki (Appendix 2). Each point is the average  $\pm 1$  standard deviation for each tephra layer (left) and for each titanomagnetite group (right). Twelve individual titanomagnetite groups are represented by colours, with empty diamonds indicating variable titanomagnetite compositions that could not be classified to any group. Bimodal titanomagnetite compositions are represented as filled triangles. Analyses in weight percent (wt%) and cation proportion (cat. prop.) calculated on the basis of four oxygen atoms as in Carmichael (1966). Major and minor element compositions of each titanomagnetite group are summarised in Table 3.2. .... 92*

**Figure 3. 7** *Glass major element compositions of Tephra Sequences A-F defined in lake and peat sediment cores from Mt. Taranaki (Appendix 3). Normalised analyses are plotted as total alkalis vs. silica with compositional fields of basalt-andesite (bA), basalt-trachyandesite (bTA), trachyandesite (TA), trachydacite (TD) and rhyolite (R).*

*Colours represent the dominant titanomagnetite group of each tephra sequence (refer to Figs. 3.6, 3.9). ..... 95*

**Figure 3. 8** *All glass compositional data from Tephra Sequence A-F summarised on plots of total alkali,  $FeO_{total}$ , CaO vs.  $SiO_2$ . The Taupo volcano-tephras (i.e., Stent, Kawakawa, Okaia) are also shown. Colours represent the dominant titanomagnetite group of each tephra sequences (refer to Figs. 3.6, 3.9). ..... 96*

**Figure 3. 9** *Summary of sediment cores taken during this study and previous studies of Turner (2008) showing individual tephra layers (thickness and depth of tephra indicated by horizontal bars; titanomagnetite group of each analysed tephra indicated by coloured bars (refer Fig. 3.6, Table 3.2); reworked tephtras are abbreviated as 'rew. '), and radiocarbon dating points given in calibrated ages (Table 3.2 and Turner, 2008). The nomenclature of individual tephra layers is based on their stratigraphic order within the composite core (refer also to Figs. 3.2 to 3.5). Tephra Sequences A-F are indicated by coloured shaded fields. Correlation of individual members and/or groups of members is indicated by black dashed lines and/or described in text. Tephra layers characterised by a bimodal titanomagnetite composition are denoted with an asterisk (refer also to Fig. 3.6). Tephra layers characterised by variable titanomagnetite compositions are denoted with brackets (refer also to Fig. 3.6). ..... 99*

**Figure 3. 10** *Lake and peat composite tephra record encompassing at least 228 tephra layers from Mt. Taranaki spanning the last 30 cal ka BP. The composite record has been constructed using the best-preserved and most-complete tephra sequences from single sites (TS = Tephra Sequence presented as colour, refer also to Figs. 3.6, 3.9) and temporal distinct tephra groups, which could be linked to the main sequence. .... 109*

**Figure 4. 1** *Brief summary of previous tephrostratigraphic work relating to eruptives of Mt. Taranaki and first correlation attempts solely based on stratigraphic position and physical properties of the deposits. The wide columns represent soil sequence records, whereas the narrow columns represent lake and peatland records. For more detailed information on the relevant tephra correlations (red shaded fields) and minor tephra correlations (dotted grey lines), as well the nomenclature of each deposit, refer to*

denoted publications. The published ages are re-calibrated using SHCal13 (Hogg et al., 2013), see text and Table 4.1 for details. Ages with asterisks derived from a key section of Alloway et al. (1995) (section 23). PDC = pyroclastic density current, NPA&BS = New Plymouth ashes and buried soils, N = north, S = south, NW = north-west, NE = north-east, SE = south-east. .... 133

**Figure 4. 2** Compositions of titanomagnetite phenocrysts from flank and ring-plain tephra deposits analysed in the current study. Each point is the average  $\pm 1$  standard deviation for each tephra unit. Each dotted field (numbered from 1-12) and colour represent an individual titanomagnetite group defined by Damaschke et al. (2017) and summarised in Table 4.3. Bi- and multi-modal titanomagnetite compositions are indicated by additional letters “-b” and “-c” after the sample name. \*E1-Konini and Mahoe (Franks et al., 1991) = Kaponga and Konini (Alloway et al., 1995) (refer to text. Analyses in weight percent (wt%) and cation proportion (cat. prop.) calculated on the basis of four oxygen atoms as in Carmichael (1966). All data summarized in Appendix 5..... 142

**Figure 4. 3** Glass chemistry of the flank and ring-plain tephra deposits analysed in the current study. Normalised analyses are plotted as total alkalis,  $\text{FeO}_{\text{total}}$ , and CaO vs. silica. The compositional fields (after Le Bas et al., 1986) of basalt-andesite (bA), basalt-trachyandesite (bTA), trachyandesite (TA), trachydacite (TD) and rhyolite (R) are also shown. Each point is the average  $\pm 1$  standard deviation for each tephra unit. Colours represent the titanomagnetite composition of each sample (refer to Fig. 4.3, Table 4.3). \*E1-Konini and Mahoe (Franks et al., 1991) = Kaponga and Konini (Alloway et al., 1995) (refer to text). All data summarized in Appendix 6. .... 143

**Figure 4. 4** Electron microprobe-determined titanomagnetite composition of the Manganui tephra units (MA-MF) and single Manganui tephra unit (M) from the Mangatoki Stream section shown as compositional fields and correlative lake and peat tephra layers shown as average points with  $\pm 1$  standard deviation. Note the large compositional variability of Manganui D..... 144

**Figure 4. 5** *Electron microprobe-determined compositions of titanomagnetite phenocrysts from the pyroclastic deposits at the Onaero Beach section (section-23; Alloway et al., 1995). Each dotted field (1-12) and colour represent an individual titanomagnetite group defined by Damaschke et al. (2017) summarised in Table 4.3.* 145

**Figure 4. 6** *Representation of the links between lake and peat tephra sequences, and proximal and medial tephra successions on Mt. Taranaki. Each coloured line in the lake and peat column and coloured names in the medial and proximal column indicate the titanomagnetite composition (i.e., group) of the respective tephra deposit (refer to Fig. 4.3, Table 4.3). Asterisks indicate bi- or multimodal titanomagnetite compositions. The coloured bands that link the columns indicate Tephra Sequences (TS A-F) characterised by their dominant titanomagnetite group. Dotted lines highlight specific correlations (refer to text). Age references are according to Table 4.1 and ages for the lake-and-peat composite record after Damaschke et al. (2017). Note the previous stratigraphy of Alloway et al. (1995) at the Onaero Beach section (grey-coloured names), which has been revised in the current study. ....* 157

**Figure 5. 1** *Location map of the tephra deposition sites (pv = previous studied sites by Turner et al. 2008, 2009), Cape Egmont, western North Island, New Zealand. TVZ = Taupo Volcanic Zone .....* 177

**Figure 5. 2** (A) *The rates of deposition of tephtras within lake and peat sequences recovered from six different localities at Mt. Taranaki (age data from Damaschke et al. 2017a) presented as histograms of tephtras deposited over 500 year intervals (left axis, grey columns), and annual tephra deposition rates generated using a Gaussian kernel smoother (Silverman 1984, 1986; Wand and Jones 1994, 1995) with a 100-year bandwidth (right axis, red line). Numbers indicate intervals during which particularly high rates of tephra deposition occurred. (B) Cumulative deposition of the same tephra units. Letters indicate periods of low rates of tephra deposition and/or no deposition. Yellow coloured fields represent disturbed or oxidised/dried sediment horizons. ....* 181

**Figure 5. 3** *Variation in the deposition rate of tephra layers across all sites analysed presented as histograms of tephtras deposited over 500 year intervals (left axis,*



columns), and annual tephra deposition rates generated using a Gaussian kernel smoother (Silverman 1984, 1986; Wand and Jones 1994) with a 100-year bandwidth (right axis, red line). Cumulative deposition rates are also shown. Two different matching models are presented: (A) A manually-merged composite record with conservative traditional stratigraphic matching, based on tephra appearance (individual and patterns) and geochemical matches; and (B) a statistically-combined record developed using a matching algorithm (following the approach of Green et al. 2014). Numbers indicate periods of high rates of tephra deposition and letters indicate periods where tephra deposition rates were low including two quiescence periods (A and H; marked as red-shaded fields) (refer to text). Note: HRTD intervals-3 and -4 may indicate one long-lasting high-frequency interval, since no repose times >200 years are recorded within this particular period (dotted line). LRk = Lake Rotokare, LRi = Lake Richmond, LU = Lake Umutekai, NS = Ngaere Swamp, ES = Eltham Swamp, TS = Tariki Swamp. .... 183

**Figure 5. 4** Annual tephra deposition rates of each single record in comparison with the statistically-combined record. Rates are generated using a Gaussian kernel smoother (Silverman 1984, 1986; Wand and Jones 1994) with a 100-year bandwidth. Note the offset of the Lake Rotokare events. .... 187

**Figure 5. 5** Histogram of 19,900 sampled inter-event times based on Monte Carlo simulations of the new statistically-merged Mt. Taranaki eruption record. Curves show the different densities fitted for this data set with AD1785 (red) and AD1820 (blue) as last volcanic activity events. .... 192

**Figure 5. 6** (A) Probabilities of no eruption of Mt. Taranaki occurring over future time periods, based on three models of inter-event distributions with AD1785 (red) and AD1820 (blue) as last volcanic activity events. (B) Annual eruption probabilities estimated for Mt. Taranaki, assuming the last volcanic activity event was at AD1785 (red) and AD1820 (blue). Note: The Weibull renewal distribution is similar to a simple Poisson process..... 194

**Figure 5. 7** (A) Probabilities of no eruption at Mt. Taranaki occurring over future time periods, based on the inter-event distribution constructed in each previous paper and for the statistically-combined record built in this study, with AD1800 (compromise date between AD1785 and AD1820) as last volcanic activity events. (B) Annual eruption probabilities of Mt. Taranaki estimated for different records proposed in previous studies and for the statistically-combined record built in this study, assuming the last volcanic activity event was at AD1800.. ..... 195

**Figure 6. 1** Total Alkalis vs. Silica (TAS) diagram (Le Bas et al., 1986) for the Mt. Taranaki whole-lapilli samples analysed from lake and peatland tephtras recovered in this study (Appendix 7). Compositional fields are basalt (B), basalt-andesite (bA), andesite (A), trachybasalt (TB), basalt-trachyandesite (bTA), and trachyandesite (TA). All analyses are on a water-free basis. Colours represent the titanomagnetite group of each tephra sample (refer also to Fig. 6.8 and Chapter 3). Dotted line represents the alkaline/subalkaline compositional boundary. .... 216

**Figure 6. 2** Total Alkalis vs. Silica (TAS) diagram (Le Bas et al., 1986) and selected  $\text{SiO}_2$  variation diagrams (with  $\text{K}_2\text{O}$  v.s  $\text{SiO}_2$  after LeMaitre et al., 2002) illustrating variation in the whole-lapilli major and trace elements for the Mt. Taranaki tephra sequences (A-F) from the lake and peat cores (Chapter 3). Whole-rock analyses of lava flows, pyroclastic flows and fall deposits (references as in figure) are also shown for comparison. All analyses are on a water-free basis with total iron presented as  $\text{Fe}_2\text{O}_3$ . Compositional fields are basalt (B), basalt-andesite (bA), andesite (A), dacite (D), trachybasalt (TB), basalt-trachyandesite (bTA), trachyandesite (TA), and trachydacite (TD). Dotted ellipsoids indicate contrasting whole-lapilli sample compositions (referred to in the text). .... 217

**Figure 6. 3** Normalised trace element diagrams for the Mt. Taranaki whole-lapilli samples with the normalised values from Sun and McDonough (1989). Individual tephra samples are classified within their tephra sequence (A-F) represented by different colours (see Chapter 3). .... 219



**Figure 6. 4** Glass compositional variations of the alkalis,  $\text{Al}_2\text{O}_3$ ,  $\text{CaO}$ ,  $\text{MgO}$ ,  $\text{FeO}$ , and  $\text{TiO}_2$  vs.  $\text{SiO}_2$  abundances for the Mt. Taranaki distal and proximal tephtras (compiled in Chapters 3 and 4; Damaschke et al. 2017a, 2017b) compared with model fractional crystallisation paths represented by the series of black spots, which mark 5% crystallisation steps (see Table 6.2). All analyses are normalised to 100% and each point is the average  $\pm 1$  standard deviation for each tephra sample.  $\text{FeO}$  is determined as total iron. Also shown are the compositions of common mineral phases (plag = plagioclase, amph = amphibole, cpx = clinopyroxene) in Mt. Taranaki volcanic rocks (Turner et al., 2008a) and xenoliths (coloured shaded fields that correspond to their respective minerals; Gruender, 2006, Gruender et al., 2010). ..... 223

**Figure 6. 5** Titanomagnetite compositional variations of  $\text{MgO}$  and  $\text{Fe}^{3+}$  vs.  $\text{TiO}_2$ ,  $\text{Fe}^{2+}$  vs.  $\text{Fe}^{3+}$ , and  $\text{Al}_2\text{O}_3$  vs.  $\text{MgO}$  abundances for the Mt. Taranaki distal and proximal tephtras (compiled in Chapters 3 and 4; Damaschke et al. 2017a, 2017b). All analyses are in weight percent and the cation proportion (cat. prop.) is calculated on the basis of four oxygen atoms as in Carmichael (1966). Each point is the average  $\pm 1$  standard deviation for each tephra sample. Two compositional trends are highlighted by solid arrows alongside the plotted trends, and secondary trends are indicated by dotted arrows (refer to text, 6.5.3.2). ..... 224

**Figure 6. 6** Minor and trace element titanomagnetite variation as function of Mg abundances (latter is based on microprobe data) for Mt. Taranaki lake and peatland tephra layers. All analyses are in parts per million (ppm) with Mg as cation proportion (cat. prop.) calculated on the basis of four oxygen atoms as in Carmichael (1966). Colours represent different tephra sequences and their respective dominant titanomagnetite group (see Chapter 3). ..... 225

**Figure 6. 7** Time-series glass (gl) and whole-lapilli (wl) compositional trends observed within distal and proximal tephra deposits of Mt. Taranaki. Bulk-analyses of young lava flows, including the Summit and Fanthams Peak lavas (Stewart et al., 1996; Price et al., 1999), are also shown so as to complete the youngest time-frame of emplacement. All analyses are on a water-free basis with total iron as  $\text{Fe}_2\text{O}_3$  in bk, and  $\text{FeO}$  in gl. Each point is the average  $\pm 1$  standard deviation for each tephra layer within the gl. Note:

*Tephra Sequence F is stratigraphically separated from the rest of the tephra sequences by a ~6000 cal yr BP depositional hiatus (for more information see Chapter 3). ..... 228*

**Figure 6. 8** *Time-series titanomagnetite compositional trends observed within distal and proximal tephra deposits of Mt. Taranaki. All analyses are weight percent and cation proportion (cat. prop.) is calculated on the basis of four oxygen atoms as in Carmichael (1966). Each tephra (each point = average +1 standard deviation) is indicated by its respective tm-group (see colour). Only tephras from the composite record are shown (Chapter 3 and 4). Triangles represent tephras with bimodal compositions. (sub-population is indicated by ellipsoid; referred to in text). Note: Tephra Sequence F is stratigraphically separated from the rest of the tephra sequences by a ~6000 cal yr BP depositional hiatus (for more information see Chapter 3). ..... 230*

**Figure 6. 9** *Major element glass (gl) vs. titanomagnetite (tm) abundances, and MgO whole-lapilli (wl) vs. MgO titanomagnetite (tm) abundances for Mt. Taranaki tephras. Diamonds represent lake and peat tephras (Damaschke et al., 2017a) and circles represent proximal tephra deposits (Damaschke et al., 2017b). ..... 237*

